

# Oscillatory and Excitable Dynamics in an Opinion Model with Group Opinions

Corbit R. Sampson and Juan G. Restrepo

*Department of Applied Mathematics, University of Colorado at Boulder, Colorado 80309, USA*

Mason A. Porter

*Department of Mathematics, University of California,  
Los Angeles, California 90095, USA; Department of Sociology,  
University of California, Los Angeles, California 90095,  
USA; and Santa Fe Institute, Santa Fe, New Mexico 87501, USA*

(Dated: August 27, 2024)

In traditional models of opinion dynamics, each agent in a network has an opinion and changes in opinions arise from pairwise (i.e., dyadic) interactions between agents. However, in many situations, groups of individuals can possess a collective opinion that may differ from the opinions of the individuals. In this paper, we study the effects of group opinions on opinion dynamics. We formulate a hypergraph model in which both individual agents and groups of 3 agents have opinions, and we examine how opinions evolve through both dyadic interactions and group memberships. In some parameter regimes, we find that the presence of group opinions can lead to oscillatory and excitable opinion dynamics. In the oscillatory regime, the mean opinion of the agents in a network has self-sustained oscillations. In the excitable regime, finite-size effects create large but short-lived opinion swings (as in social fads). We develop a mean-field approximation of our model and obtain good agreement with direct numerical simulations. We also show, both numerically and via our mean-field description, that oscillatory dynamics occur only when the number of dyadic and polyadic interactions per agent are not completely correlated. Our results illustrate how polyadic structures, such as groups of agents, can have important effects on collective opinion dynamics.

## I. INTRODUCTION

The opinions of individuals in a social network often change when they are exposed to the opinions and actions of other individuals. The ensuing evolution, which is the *opinion dynamics*, of the individuals in a network, has received considerable attention from sociologists [1], economists [2], political scientists [3, 4], applied mathematicians and theoretical physicists [3, 5–8], and many others. Researchers have studied models of opinion dynamics on social networks to gain insight into phenomena such as the propagation of false or misleading information [9, 10], the emergence of consensus opinions [7, 11, 12], and the formation of echo chambers [13, 14]. See [15, 16] for reviews of opinion models.

Models of opinion dynamics necessarily involve many assumptions about the nature of the opinions of individuals, interactions between individuals, and how such interactions affect the opinions of other individuals [17]. Most opinion models assume that agent opinions change when the agents interact with each other in a pairwise (i.e., dyadic) fashion. The opinions of the agents are typically either real-valued scalars or real-valued vectors (e.g., if one wants to simultaneously model opinions on multiple things). In some models, the opinions have discrete values; in others, they have continuous values, such as in an interval of the real line. There are a wealth of opinion models [16, 18], which researchers study on networks to examine how social structures affect opinion dynamics. Examples of opinion models include the DeGroot consensus model [19], voter models [20, 21] and their generalizations [22], majority-rule models [23], and

bounded-confidence models [24].

A basic assumption in most opinion models is that only the individual agents, which are represented by the nodes of a network, are endowed with an opinion. In the present paper, we relax this assumption by allowing groups of nodes to hold a collective opinion. Social groups, which range from basic family and friendship units to large political and corporate organizations, help shape the fabric of society [25–27]. In many situations, it is reasonable to posit that social groups themselves can possess opinions. For example, large corporate organizations sometimes take public stances on social issues [28]. Additionally, courts such as the United States Supreme Court hear cases and document collective opinions through their decisions on these cases [29]. Moreover, a mathematics department at a university may broadcast a collective opinion, such as through documentation on its website or a faculty hiring decision, that differs markedly from the opinions of its individual faculty. The opinion of a research group, such as the applied-mathematics group, may also differ from the individual opinions of members of that group. In all of these examples, a group’s opinion does not necessarily reflect a consensus among the members of that group, as individual members of the group can disagree (sometimes rather strongly) with the group opinion. Importantly, however, groups and individual members of a group mutually influence each other. Group opinions are influenced by the opinions of its constituent members, and the opinions of individuals are influenced by the opinions of the groups to which they participate [30, 31].

In the present paper, we formulate and analyze a model

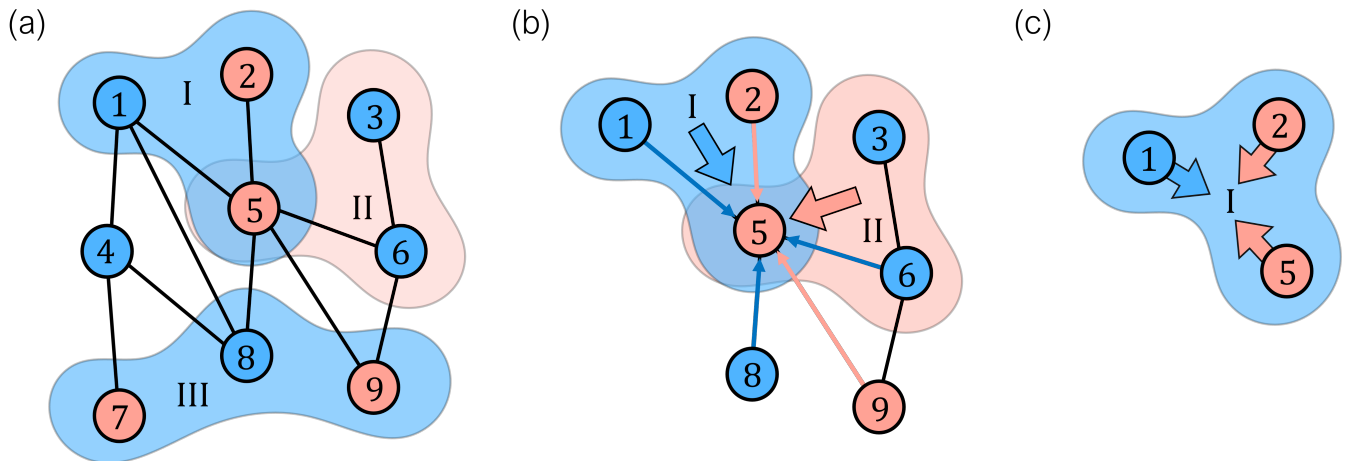


FIG. 1: A schematic illustration of how the opinions of nodes and groups are influenced by the opinions of other nodes and groups in our model. (a) A hypergraph with 9 nodes and 3 groups. Nodes 1, 3, 4, 6, and 8 have opinion 1 [in blue], and nodes 2, 5, 7, and 9 have opinion 0 [in light red]. Groups I and III have opinion 1 [in blue], and group II has opinion 0 [in light red]. (b) Node 5’s opinion is influenced by the opinion of its neighboring nodes 1, 2, 6, 8, and 9 [thin arrows] and by the opinions of groups I and II [thick arrows]. (c) Group I’s opinion is influenced by the opinions of its constituent nodes 1, 2, and 5 [thick arrows].

of opinion dynamics in which both a network’s nodes and its groups of nodes have a binary opinion. The opinions of individual nodes are affected both by their neighbors in a network and by the opinions of the groups to which they participate. The opinions of groups are affected by the opinions of its constituent nodes. For simplicity, we neglect interactions between distinct groups. In Fig. 1, we give a schematic illustration of how the opinions of nodes and groups are influenced by the opinions of other nodes and groups in our model, which we describe in detail in Sec. II A. In our model, group opinions can lead, depending on the parameter values, to oscillatory opinion dynamics and to excitable opinion dynamics. In the oscillatory regime, the mean opinion of a network develops self-sustained oscillations. In the excitable regime, a situation in which most of the nodes have the same opinion can quickly and temporarily change to a situation in which most nodes have the other opinion. The emergence of these regimes depends strongly on the correlation between group structure and dyadic network adjacencies. We develop a mean-field approximation of our model’s dynamics and use it to gain insight into its dynamics. We find that the onset of excitable dynamics occurs due to a bifurcation from a stable equilibrium into sustained oscillatory dynamics. This bifurcation resembles the onset of excitable dynamics in models of neuronal dynamics [32, 33]. We also note the qualitative similarity between the excitable dynamics of our model and the formation of social fads, which is a collective behavior in which a topic, object, or behavior experiences an increase in popularity that forms suddenly, lasts a short amount of time, and declines rapidly [34, 35].

The role of group interactions, which are often called “higher-order interactions” and “polyadic interactions”,

in opinion dynamics and other dynamical processes on networks has received much attention in the past few years [36–38]. The renewed interest on polyadic interactions in complex systems has built on foundational work that dates back many decades [39–42]. In social systems, there is much recent work on extending models to incorporate polyadic interactions [5, 7, 8, 11, 12, 43–51]. In these extensions, the opinions are associated with individual agents and they change due to both pairwise and group interactions. By contrast, in our generalization, we also assign opinions to the groups themselves. In this sense, our work is similar to recent efforts that examined the synchronization of quantities that are defined on the edges and higher-order simplices of a simplicial complex [52–54].

The incorporation of polyadic interactions into network dynamics can significantly affect qualitative behavior. For example, “opinion jumping” can occur in polyadic bounded-confidence models [8] and bistable regions can arise in polyadic models of disease spread [43, 44, 55]. Similarly, the nature of the synchronization transition of phase oscillators can change qualitatively when one incorporates polyadic interactions [56, 57]. Our observation that group opinions can induce oscillatory and excitable dynamics provides another example of how polyadic interactions can fundamentally modify the dynamics of networked systems.

Our paper proceeds as follows. In Sec. II, we introduce our stochastic opinion model and discuss the random-hypergraph model on which we simulate opinion dynamics. In Sec. III, we derive a mean-field description of our model and discuss the approximations that we make to study the steady-state behavior of our system. In Sec. IV, we discuss the formation of group–node discordance

states. In Sec V, we examine the formation of excitable and oscillatory dynamics. Finally, in Sec. VI, we summarize and discuss our findings. Our code, figures, and, data are available at [https://github.com/CorbitSampson/Oscillatory\\_Excitable\\_Opinion\\_Dynamics.git](https://github.com/CorbitSampson/Oscillatory_Excitable_Opinion_Dynamics.git).

## II. OUR STOCHASTIC OPINION MODEL AND RANDOM HYPERGRAPHS

### A. Stochastic opinion model

In this section, we describe our model of opinion dynamics with group opinions. We consider a set  $V$  of  $N$  nodes, which we index by  $i \in \{1, 2, \dots, N\}$ . Each node holds a binary opinion, which is either 0 or 1. Our model uses discrete time, so the time  $t \in \{0, 1, \dots\}$  and node opinions update synchronously using the opinions of the nodes and the groups at the previous time step. Let  $x_i^t$  denote the opinion of node  $i$  at time  $t$ . As in models of opinion dynamics on ordinary graphs, which assume dyadic interactions between nodes, our nodes are adjacent to each other if there is an edge between them in a graph  $G$ , which has an associated adjacency matrix  $A$ . We assume that  $G$  is undirected and unweighted, so  $A_{ij} = A_{ji} = 1$  if nodes  $i$  and  $j$  are adjacent and  $A_{ij} = A_{ji} = 0$  if they are not adjacent. We also consider a set of  $S$  groups of nodes (i.e., subsets of  $V$ ) of size 3. Each group also has either opinion 0 or opinion 1. We label the groups with the index  $j \in \{1, 2, \dots, S\}$ , and we denote the opinion of group  $j$  at time  $t$  by  $y_j^t$ . As with node opinions, group opinions update synchronously using the state of the system at the previous time. The  $N \times S$  incidence matrix  $M$  has entries  $M_{ij} = 1$  if node  $i$  participates in group  $j$  and  $M_{ij} = 0$  if it does not. Our model only allows 3-node groups to hold an opinion, but one can also consider models in which 2-node groups (i.e., dyads) hold opinions. We do this to emphasize our model's key novel feature (namely, group opinions) in a way that separates it from traditional considerations (namely, dyadic interactions and the associated edges of a network).

In our opinion model, the opinion of a node is influenced both by the opinions of the adjacent nodes (i.e., dyadic influence) and by the opinions of the groups in which it participates (i.e., polyadic influence) [see Fig. 1(b)]. The opinion of a group is influenced by the opinions of its constituent nodes [see Fig. 1(c)]. For simplicity, we suppose that all groups have exactly 3 nodes, although this is certainly interesting to generalize to groups with other sizes and heterogeneous sizes. This case already yields extremely rich dynamics and illustrates key differences between our model and previous models (which do not have group opinions). Given this assumption, we henceforth refer to groups in our networks as “triangles”. Let  $\langle k^{(2)} \rangle = \sum_{i,j} A_{ij}/N$  and  $\langle k^{(3)} \rangle = \sum_{i,j} M_{ij}/N$ , respectively, denote the mean numbers of edges and triangles per node of a network.

We now describe our model in detail. The opinions of the nodes and triangles evolve stochastically according to the update rule

$$x_i^{t+1} = \begin{cases} 1 & \text{with probability } p_i^N(\mathbf{x}^t, \mathbf{y}^t) \\ 0 & \text{otherwise,} \end{cases} \quad (1)$$

$$y_j^{t+1} = \begin{cases} 1 & \text{with probability } p_j^E(\mathbf{x}^t, \mathbf{y}^t) \\ 0 & \text{otherwise,} \end{cases} \quad (2)$$

where  $\mathbf{x}^t = [x_1^t, x_2^t, \dots, x_N^t]^T$  is a node opinion vector and  $\mathbf{y}^t = [y_1^t, y_2^t, \dots, y_S^t]^T$  is a triangle opinion vector.

Suppose that the probability that node  $i$  adopts opinion 1 is a sigmoidal function of a linear combination of the opinions of its adjacent nodes (via its incident edges) and the opinions of the triangles (i.e., groups) in which it participates. That is,

$$p_i^N(\mathbf{x}^t, \mathbf{y}^t) = f_N(a\bar{x}_i^t + b\bar{y}_i^t), \quad (3)$$

where

$$\bar{x}_i^t = \sum_{j=1}^N A_{ij} x_j^t / \langle k^{(2)} \rangle, \quad (4)$$

$$\bar{y}_j^t = \sum_{k=1}^S M_{jk} y_k^t / \langle k^{(3)} \rangle, \quad (5)$$

the function  $f_N$  is a sigmoidal function, and  $a$  and  $b$  are real-valued constants. The parameter  $a$  encodes the influence of node opinions on their neighbors, and the parameter  $b$  encodes the influence of triangle opinions on their constituent nodes, as we will discuss in more detail below. In our update rule, nodes do not consider their own current opinions when they update their opinions. We discuss this choice in more detail shortly.

Suppose that the probability that a triangle adopts opinion 1 is a sigmoidal function of a linear combination of the opinion of its constituent nodes and its own current opinion. That is,

$$p_j^E(\mathbf{x}^t, \mathbf{y}^t) = f_E(c\bar{z}_j^t + d y_j^t), \quad (6)$$

where

$$\bar{z}_j^t = \frac{1}{3} \sum_{i=1}^N M_{ij} x_i^t, \quad (7)$$

where  $f_E$  is a sigmoidal function and  $c$  and  $d$  are real-valued constants. The parameter  $c$  encodes the influence of node opinions on the triangles to which they belong, and the parameter  $d$  encodes the tendency of a triangle to maintain its opinion. For simplicity, we use the same sigmoidal function for all nodes and all triangles, so

$$\begin{aligned} f(z) &:= f_N(z) = f_E(z) \\ &= \frac{1}{2} [1 + \tanh(m(z - \mu))], \end{aligned} \quad (8)$$

where  $\mu$  is the inflection point of the sigmoid  $f(z)$  and  $1/m$  is proportional to the width of the sigmoid’s transition region. We use a sigmoidal function because it is convenient for representing saturating interactions [58]. Researchers have used sigmoidal functions in many other models, including models of echo chambers and polarization [13], smooth bounded-confidence models [14], and more generally in many other saturating interactions, which occur in diverse fields that range from neuroscience to robotics [59].

In our simulations of the stochastic opinion model (1)–(2), the initial opinion of each node and each triangle is either 0 or 1. Each node initially has opinion 1 with probability  $u_1$  and opinion 0 with probability  $1 - u_1$ , and each triangle initially has opinion 1 with probability  $u_2$  and 0 with probability  $1 - u_2$ . For the remainder of this article, we specify the initial conditions of the stochastic opinion model (1)–(2) as ordered pairs  $(u_1, u_2)$ .

As we highlighted above, we assume that individual nodes do not account for their own current opinions when they update their opinions. We do this to emphasize the role of social interactions — both dyadic and polyadic — in the opinion-formation process. Essentially, we are examining a regime in which the effects of self-influence are small in comparison to the effects of social interaction. In this respect, our opinion model is very different from many opinion models [16], but it follows the tradition of classical voter models [20–22]. However, we do allow groups to influence themselves. This allows us to model the effects of social phenomena, such as “pluralistic ignorance” [60, 61] and “groupthink” [62], that can slow down changes in group opinions. In pluralistic ignorance, the members of a group incorrectly believe that they hold a minority opinion within a group [60, 61]. Pluralistic ignorance, which one can view as a “minority illusion” [63] in social dynamics, provides a potential mechanism to slow social change through a process of self-silencing, such that individuals appear to conform to a belief that they believe is held by the rest of a group [64]. Groupthink refers to the desire of individuals in a group to seek social conformity and thereby disregard their own opinions. Our opinion model does not directly encode pluralistic ignorance or groupthink, but one can view its group self-influence term (which dampens changes in group opinions) as incorporating them indirectly.

In Table I, we summarize the parameters of our model. The parameters  $a$  and  $b$  encode how much nodes are influenced by their neighboring nodes (the parameter  $a$ ) and by the groups in which they participate (the parameter  $b$ ). In particular,  $a > 0$  (respectively,  $a < 0$ ) increases (respectively, decreases) the probability that a node transitions to or maintains opinion 1 when more of its neighbors have opinion 1. Analogously,  $b > 0$  (respectively,  $b < 0$ ) increases (respectively, decreases) the probability that a node transitions to or maintains opinion 1 as it participates in more groups with opinion 1. Positive (respectively, negative) values of the parameters  $c$  and  $d$  increase (respectively, decrease) the probability that a

TABLE I: The parameters of our opinion model.

Parameter	Definition
$a$	The influence of individuals on other individuals
$b$	The influence of groups on individuals
$c$	The influence of individuals on groups
$d$	The influence of a group’s opinion on itself
$f$	Sigmoidal influence function
$\mu$	Inflection point of the sigmoid $f$
$1/m$	Width of the transition of the sigmoid $f$
$r$	The correlation coefficient between dyadic degree and triadic degree
$\mathcal{P}$	The hyperdegree distribution
$P_1$	The marginal dyadic degree distribution
$P_2$	The marginal triadic degree distribution
$k$	Dyadic degree (i.e., ordinary node degree)
$q$	Triadic degree

group transitions to or maintains opinion 1 based on the fraction of its nodes with opinion 1 and its own current opinion, respectively. Therefore, we interpret positive values of the parameters  $a$ ,  $b$ ,  $c$ , and  $d$  as conforming to influence, and we interpret negative values of these parameters as rejecting influence. If  $a + b < \mu$ , the argument of  $f_N(\cdot)$  in Eq. (3) is typically less than  $\mu$  for nodes with hyperdegree close to the mean hyperdegree, so the opinions of nodes tend to be biased towards opinion 0. However, nodes with sufficiently large hyperdegree may not experience this bias. Analogously, if  $c + d < \mu$ , then the opinions of triangles (i.e., groups) tend to be biased towards opinion 0.

## B. Random-hypergraph model

It is convenient to use hypergraphs to describe our networks, which consist of nodes and groups of nodes. A hypergraph is a generalization of a graph that includes both ordinary edges (i.e., dyadic adjacencies) and hyperedges with more than two nodes (i.e., polyadic adjacencies) [36, 37, 65]. Following standard convention, we refer to any of these adjacencies as hyperedges. Mathematically, a hypergraph  $\mathcal{H} = (V, E)$  consists of a set  $V$  of nodes and a set  $E$  of hyperedges. Each hyperedge is a nonempty subset of  $V$ ; the number of nodes in this subset is the “size” of the hyperedge. In an ordinary graph, each node  $i \in V$  has an associated degree  $k_i$ , which indicates the number of edges that are attached (i.e., “incident”) to it. In a hypergraph, the hyperdegree of node  $i$  is the vector  $\mathbf{k}_i = [k_i^{(2)}, k_i^{(3)}, \dots, k_i^{(D)}]$ , where  $D$  is the size of its largest hyperedge and the  $m$ th-order degree  $k_i^{(m)}$  is the number of size- $m$  hyperedges that are incident to node  $i$ . Each hypergraph has a hyperdegree distribution  $\mathcal{P}(\mathbf{k})$ , which encodes the probabilities that a uniformly-randomly-chosen node has hyperdegree  $\mathbf{k}$  for each  $\mathbf{k}$ .

Just as one can describe a hypergraph using a bipartite network [65], it is also possible to formulate our model by considering dynamics on an ordinary graph with two types of nodes. In this formulation, the agents constitute one type of node and the groups constitute a second type of node. The agents can have adjacencies both with groups and with other agents, and the groups are adjacent to each agent that participates in the group. We view the group language is much more natural, just as the language of hypergraphs and simplicial complexes is natural for studying polyadic interactions [37, 66].

To study our opinion model, it is convenient to use random hypergraphs with specified hyperdegree sequences. We now describe the particular random-hypergraph model that we employ. Suppose that we have a set of nodes  $i \in \{1, 2, 3, \dots, N\}$  with hyperdegree  $\mathbf{k}_i$ , where  $k_i^{(m)}$  is the number of loose ends (i.e., “stubs”) for size- $m$  hyperedges that are attached to  $i$ . We form a size- $m$  hyperedge by uniformly randomly selecting  $m$  stubs for the hyperedge. We repeat this stub-selection process until all stubs are assigned to a hyperedge. The resulting probability that there is a size- $m$  hyperedge that connects nodes  $\{i_1, i_2, \dots, i_m\}$  is [67]

$$f_m(\mathbf{k}_{i_1}, \mathbf{k}_{i_2}, \dots, \mathbf{k}_{i_m}) = \frac{(m-1)! k_{i_1}^{(m)} k_{i_2}^{(m)} \dots k_{i_m}^{(m)}}{(N \langle k^{(m)} \rangle)^{m-1}}. \quad (9)$$

This random-hypergraph model is convenient because it allows us to control the degree sequence of a hypergraph. It also allows us to model situations with correlations between the degrees of different orders (i.e., describing situations in which nodes with many dyadic connections are also likely to participate in many groups) or anti-correlated. As we discussed previously, we only consider groups of size 3. Therefore, our hypergraphs have hyperedges of sizes 2 (i.e., edges) and 3 (i.e., triangles), and each node is characterized by its 2nd-order degree (i.e., dyadic degree) and 3rd-order degree (i.e., triadic degree), which we henceforth denote by  $k := k_i^{(2)}$  and  $q := k_i^{(3)}$ , respectively.

The above random-hypergraph model is a special case of the stub-labeled hypergraph configuration model in [68] in which we allow only hyperedges of sizes 2 and 3. When constructing a hypergraph with a configuration model, one obtains a small number of self-hyperedges and multi-hyperedges. (See [69] for relevant discussions in the context of graphs.) We retain these self-hyperedges and multi-hyperedges. Our random-hypergraph model is reminiscent of the closely related random-graph models with clustering that were proposed independently by Newman [70] and Miller [71]. In a Newman–Miller model, nodes have specified dyadic and triangle (i.e., triadic) degree sequences, which one uses independently in a stub-matching procedure. However, a Newman–Miller “triangle” yields three dyadic interactions, rather than a single size-3 hyperedge.

The formation of hyperedges in this random-hypergraph model depends only on the specified hyper-

degree of each node, so one can employ hyperdegree-based compartmental models when studying dynamical processes on hypergraphs that it generates. Such techniques have been used extensively in the study of disease spread on networks [72, 73].

To explore the effects of hyperdegree heterogeneity and correlations between the dyadic degree  $k$  and triadic degree  $q$ , we consider a convenient family of hyperdegree distributions. Given the marginal degree distributions  $P_1(\cdot)$  and  $P_2(\cdot)$  for the edges and triangles, respectively, there are two extremes for the joint distribution  $\mathcal{P}(k, q)$ . In the completely correlated case, which satisfies  $\mathcal{P}(k, q) = P_1(k)\delta(k-q)$ , the dyadic degree and triadic degree of each node is the same. In the uncorrelated case,  $\mathcal{P}(k, q) = P_1(k)P_2(q)$ , so the dyadic and triadic degrees are independent of each other. To systematically explore the effects of correlation between the dyadic and triadic degrees, we use a hyperdegree distribution that interpolates between these two extremes. This joint distribution is

$$\mathcal{P}(k, q) = P_1(k)P_2(q)(1-r) + P_1(k)\delta(q-k)r, \quad (10)$$

where the Pearson correlation coefficient  $r \in [0, 1]$  between the dyadic and triadic degrees parameterizes the amount of correlation between these degrees. When  $r = 0$ , the dyadic degree  $k$  and triadic degree  $q$  are uncorrelated; when  $r = 1$ , we have that  $k = q$  for every node.

To examine the effects of degree heterogeneity, suppose that the degree distributions  $P_1(k)$  and  $P_2(q)$  have the approximate power-law form

$$P_1(k) = P_2(k) = P(k) = \begin{cases} \left(\frac{\gamma-1}{k_{\min}^{1-\gamma}}\right) k^{-\gamma}, & k \geq k_{\min} \\ 0, & \text{otherwise,} \end{cases} \quad (11)$$

where  $k_{\min}$  is the minimum degree. In a particular hypergraph that we construct using our random-hypergraph model, we generate the hyperdegree of each node using bivariate inverse sampling from the distribution that is described by Eqs. (10) and (11). We then construct the hypergraph using the stub-matching process that we described above.

### III. MEAN-FIELD APPROXIMATION

We develop a mean-field description that approximates the dynamics of our model. Our mean-field description tracks the dynamics of three order parameters: the expected fraction  $Y^t$  of triangles at time  $t$  with opinion 1, the expected fraction  $V^t$  of nodes at time  $t$  with opinion 1 in an edge chosen uniformly at random, and the expected fraction  $U^t$  of nodes at time  $t$  with opinion 1 in a triangle chosen uniformly at random. We express the order parameters  $V^t$  and  $U^t$  in terms of  $x_{\mathbf{k}}^t$ , which is the fraction of nodes at time  $t$  with hyperdegree  $\mathbf{k} = [k, q]$

that have opinion 1. The total numbers of edges and tri-

angles are  $N\langle k\rangle/2$  and  $N\langle q\rangle/3$ , respectively, so we can write

$$V^t = \sum_{\mathbf{k}} \sum_{\mathbf{k}'} \frac{N\mathcal{P}(\mathbf{k})N\mathcal{P}(\mathbf{k}')}{2!} \left( \frac{kk'}{N\langle k\rangle} \right) \left( \frac{x_{\mathbf{k}}^t + x_{\mathbf{k}'}^t}{2} \right) / \left( \frac{N\langle k\rangle}{2} \right) = \sum_{\mathbf{k}} \frac{k\mathcal{P}(\mathbf{k})x_{\mathbf{k}}^t}{\langle k\rangle}, \quad (12)$$

where  $N\mathcal{P}(\mathbf{k})N\mathcal{P}(\mathbf{k}')/2!$  is the expected number of pairs of nodes with hyperdegrees  $\mathbf{k}$  and  $\mathbf{k}'$ , the quantity  $kk'/(N\langle k\rangle)$  is the expected fraction of these pairs that are connected by an edge [see Eq. (9) with  $m = 2$ ], and  $(x_{\mathbf{k}}^t + x_{\mathbf{k}'}^t)/2$  is the expected fraction of opinion-1 nodes

that are attached to an edge that connects uniformly-randomly-selected nodes with hyperdegrees  $\mathbf{k}$  and  $\mathbf{k}'$ . Alternatively,  $V^t$  represents the probability that one moves to an opinion-1 node by following an edge that one chooses uniformly at random. Similarly, we can write

$$\begin{aligned} U^t &= \sum_{\mathbf{k}} \sum_{\mathbf{k}'} \sum_{\mathbf{k}''} \frac{N\mathcal{P}(\mathbf{k})N\mathcal{P}(\mathbf{k}')N\mathcal{P}(\mathbf{k}'')}{3!} \left( \frac{2qq'q''}{(N\langle q\rangle)^2} \right) \left( \frac{x_{\mathbf{k}}^t + x_{\mathbf{k}'}^t + x_{\mathbf{k}''}^t}{3} \right) / \left( \frac{N\langle q\rangle}{3} \right) \\ &= \sum_{\mathbf{k}} \frac{q'\mathcal{P}(\mathbf{k})x_{\mathbf{k}}^t}{\langle q\rangle}. \end{aligned} \quad (13)$$

Note that  $V^t$  and  $U^t$  are closely related to — but can differ from — the expected fraction  $(\sum_{\mathbf{k}} \mathcal{P}(\mathbf{k})x_{\mathbf{k}}^t)$  of nodes with opinion 1 at time  $t$ .

Because we generate hypergraphs using a configuration model, the probability that there is a hyperedge that connects a group of nodes depends only on the hyperdegrees of those nodes. We can thus use a hyperdegree-based compartmental model to obtain mean-field equations. Consider the probability [see Eq. (1)] that a node  $i$  with hyperdegree  $\mathbf{k} = [k, q]$  has opinion 1 at time  $t + 1$ . Assuming that all nodes with the same hyperdegree behave equally, we approximate  $\bar{x}_i^t$ , which is the normalized number of neighbors of node  $i$  that have opinion 1 [see Eq. (4)], by

$$\begin{aligned} \bar{x}_i^t &= \frac{1}{\langle k\rangle} \sum_{j=1}^N A_{ij} x_j^t \\ &\approx \frac{1}{\langle k\rangle} \sum_{\mathbf{k}'} N\mathcal{P}(k', q') \left( \frac{kk'}{N\langle k\rangle} \right) x_{\mathbf{k}'}^t \\ &= \frac{k}{\langle k\rangle} \sum_{\mathbf{k}'} \frac{k'\mathcal{P}(k', q')x_{\mathbf{k}'}^t}{\langle k\rangle} \\ &= kV^t / \langle k\rangle, \end{aligned} \quad (14)$$

where the approximation in the second line replaces the number of opinion-1 neighbors of node  $i$  with its expected value. The term  $\bar{y}_i^t$ , which is the normalized number of triangles that are attached to node  $i$  that have opinion 1

[see Eq. (7)], is approximately

$$\bar{y}_i^t \approx qY^t / \langle q\rangle \quad (15)$$

because node  $i$  is attached to  $q$  triangles and  $Y^t$  is the expected fraction of triangles that have opinion 1. We insert the approximations (14) and (15) into Eqs. (1)–(3) to obtain

$$\begin{aligned} x_{\mathbf{k}}^{t+1} &= \frac{1}{N\mathcal{P}(\mathbf{k})} \sum_{\mathbf{k}_i=\mathbf{k}} \mathbb{E}[x_i^{t+1}] \\ &= \frac{1}{N\mathcal{P}(\mathbf{k})} \sum_{\mathbf{k}_i=\mathbf{k}} f(a\bar{x}_i^t + b\bar{y}_i^t) \\ &\approx \frac{1}{N\mathcal{P}(\mathbf{k})} \sum_{\mathbf{k}_i=\mathbf{k}} f\left(\frac{ak}{\langle k\rangle}V^t + \frac{bq}{\langle q\rangle}Y^t\right) \\ &= f\left(\frac{ak}{\langle k\rangle}V^t + \frac{bq}{\langle q\rangle}Y^t\right), \end{aligned} \quad (16)$$

where  $\mathbb{E}[\cdot]$  denotes the expectation. The time evolution of the expected fraction  $Y^t$  of triangles with opinion 1 satisfies

$$\begin{aligned} Y^{t+1} &= \mathbb{E}\left[\frac{1}{S} \sum_{j=1}^S y_j^{t+1}\right] = \frac{1}{S} \sum_{j=1}^S \mathbb{E}[y_j^{t+1}] \\ &= \frac{1}{S} \sum_{j=1}^S \{ \mathbb{E}[y_j^{t+1} | y_j^t = 1] P(y_j^t = 1) \\ &\quad + \mathbb{E}[y_j^{t+1} | y_j^t = 0] P(y_j^t = 0) \}. \end{aligned} \quad (17)$$

Making the mean-field assumption that all triangles behave equally (i.e.,  $y_j^t = y^t$  and  $\bar{z}^t = \bar{z}_j^t$  for all  $j$ ) yields

$$Y^{t+1} = \mathbb{E}[y^{t+1}|y^t = 1]P(y^t = 1) + \mathbb{E}[y^{t+1}|y^t = 0]P(y^t = 0). \quad (18)$$

We then use Eq. (6) for the expected values and the relation  $P(y^t = 1) = Y^t$  to obtain

$$Y^{t+1} = f(c\bar{z}^t + d)Y^t + f(c\bar{z}^t)(1 - Y^t). \quad (19)$$

Finally, similarly to our approximation of  $\bar{y}_i^t$  in Eq. (15), we approximate  $\bar{z}^t$  (i.e., the fraction of nodes with opinion 1 in a triangle that we select uniformly at random) by

$$\bar{z}^t \approx U^t, \quad (20)$$

which is the expected fraction of nodes at time  $t$  with opinion 1 in a triangle that we select uniformly at random. Substituting Eq. (20) into Eq. (19) yields

$$Y^{t+1} = Y^t f(cU^t + d) + (1 - Y^t)f(cU^t). \quad (21)$$

Inserting Eq. (16) into Eqs. (12)–(13) yields a closed map for the time evolution of the three order parameters:

$$\begin{aligned} V^{t+1} &= \sum_k \sum_q \frac{kP(k, q)}{\langle k \rangle} f\left(\frac{ak}{\langle k \rangle} V^t + \frac{bq}{\langle q \rangle} Y^t\right), \\ U^{t+1} &= \sum_k \sum_q \frac{qP(k, q)}{\langle q \rangle} f\left(\frac{ak}{\langle k \rangle} V^t + \frac{bq}{\langle q \rangle} Y^t\right), \\ Y^{t+1} &= Y^t f(cU^t + d) + (1 - Y^t)f(cU^t). \end{aligned} \quad (22)$$

Because the mean-field map (22) directly describes the evolution of the three order parameters  $V^t$ ,  $U^t$ , and  $Y^t$ , we directly specify the initial conditions ( $V^0$ ,  $U^0$ , and  $Y^0$ ) of these order parameters. This contrasts with the stochastic opinion model (1)–(2), where we specify initial conditions in terms of the probabilities  $u_1$  and  $u_2$  of assigning opinion 1 to nodes and triangles, respectively. In examples that compare simulations of (1)–(2) and (22), we let  $V^0 = U^0 = u_1$  and  $Y^0 = u_2$  to make the initial conditions as similar as possible. We make this choice because the order parameters  $V^t$  and  $U^t$  are related (but not equal) to the fraction of nodes with opinion 1 [See Eqs. (12) and (13)] and  $Y^t$  is the expected fraction of triangles with opinion 1.

The mean-field description (22) relies on various approximations, which we now summarize and discuss. First, our mean-field description is a hyperdegree-based compartmental model, so it assumes that the expected time evolution of all nodes with hyperdegree  $\mathbf{k}$  is the same. (For example, the probability that each such node has opinion 1 at time  $t$  is  $x_{\mathbf{k}}^t$ .) This approximation relies on the fact that, by construction, we treat all nodes of hyperdegree  $\mathbf{k}$  as possessing the same type and number of expected connections. Our mean-field description also assumes that each node has enough connections

(through both edges and triangles) that we can replace the variables  $\bar{x}_i^t$ ,  $\bar{y}_i^t$ , and  $\bar{z}_i^t$  by their means [as we did in Eqs. (14), (15), and (20)]. In particular, we do not expect our mean-field approximation to give a good approximation for sparse hypergraphs. One can generalize our mean-field description to account for hypergraph models (e.g., degree-assortative random hypergraphs [68]) in which nodes have intrinsic variables and connect to each other with probabilities that depend on these variables. Such generalizations of configuration models have a long history of success in investigations of dynamical processes on graphs [74].

### A. Steady-state solutions of Eqs. (1)–(2)

We now examine the steady-state solutions (i.e., states in which the dynamical quantities  $V^t$ ,  $U^t$ , and  $Y^t$  are constant) of the stochastic opinion model (1)–(2) by studying the fixed points of the mean-field equations (22). We obtain qualitatively similar steady-state solutions and bifurcations for any value of the hyperdegree correlation  $r \in [0, 1]$ . Therefore, for simplicity, we assume in the present discussion that  $r = 1$ , which implies that the dyadic degree and triadic degree are perfectly correlated (i.e.,  $k = q$ ). We use this assumption for the remainder of this section and throughout Sec. IV. We will see in Sec. V that relaxing this assumption results in qualitatively different dynamics. Under this assumption,  $V^t = U^t$  and the mean-field equations (22) reduce to

$$\begin{aligned} V^{t+1} &= \sum_k \frac{kP(k)}{\langle k \rangle} f\left(\frac{k}{\langle k \rangle} (aV^t + bY^t)\right), \\ Y^{t+1} &= Y^t f(cV^t + d) + (1 - Y^t)f(cV^t). \end{aligned} \quad (23)$$

Any fixed point  $[V^t, Y^t] = [V^*, Y^*]$  of the map (23) must satisfy

$$V^* = \sum_k \frac{kP(k)}{\langle k \rangle} f\left(\frac{k}{\langle k \rangle} (aV^* + bY^*)\right), \quad (24)$$

$$Y^* = Y^* f(cV^* + d) + (1 - Y^*)f(cV^*). \quad (25)$$

Solving (25) for  $Y^*$  and substituting the result into Eq. (24) shows that the fixed points of Eqs. (23) have the form  $[V^*, Y^*] = [F(V^*), G(V^*)]$ , where

$$\begin{aligned} F(V) &= \sum_k \frac{kP(k)}{\langle k \rangle} f\left(\frac{k}{\langle k \rangle} (aV + bG(V))\right), \\ G(V) &= \frac{f(cV)}{1 + f(cV) - f(cV + d)}. \end{aligned} \quad (26)$$

The equation  $V^* = F(V^*)$  is a one-dimensional equation for  $V^*$  that one can solve using a root-finding algorithm. After determining  $V^*$ , we obtain  $Y^*$  using the equation  $Y^* = G(V^*)$ .

To illustrate the usefulness of Eqs. (24)–(25) to study steady-state solutions of the original stochastic opinion

model (1)–(2), we compare the fixed points that we obtain from the solution of Eqs. (24)–(25) with the results of simulations of Eqs. (1)–(2). In Fig. 2, we plot both the steady-state values  $V^*$  and  $Y^*$  that we obtain from simulations of Eqs. (1)–(2) (dots) and the fixed-point solutions of Eqs. (24)–(25) (solid and dashed curves) as a function of the sigmoid inverse-width parameter  $m$  for  $a = b = c = d = \mu = 1/2$  and power-law exponent  $\gamma = 4$ . Because  $a$ ,  $b$ ,  $c$ , and  $d$  all have positive values, all nodes and groups experience only conforming influence. For each value of  $m$ , we iterate Eqs. (1)–(2) for 400 steps and plot the values of  $V^*$  and  $Y^*$  after the final step. We do 100 independent simulations of this process with initial conditions  $(u_1, u_2)$  spaced evenly in the unit square (i.e.,  $\{(i/9, j/9) | i \in \{0, 1, \dots, 9\}, j \in \{0, 1, \dots, 9\}\}$ ). For each value of  $m$ , we use the same hypergraph with  $N = 700$  nodes. Both our simulations of the stochastic opinion model (1)–(2) and our analysis of the reduced mean-field approximation (23) illustrate that the system transitions from a monostable to a bistable regime as we increase  $m$ . Although we observe some quantitative differences between our mean-field solutions and our direct simulations, the fixed points of the mean-field equations are reasonably successful at approximating the steady-state solutions of the original stochastic opinion model. The bifurcation in Fig. 2 gives an interesting example of the behavior of our model. A similar bifurcation was also observed in another opinion model with sigmoidal interactions [59]. Therefore, we do not focus on such bifurcations of steady-state solutions in situations with perfectly correlated dyadic and triadic degrees (i.e.,  $r = 1$ ). Instead, we investigate novel features that arise due to the presence of group opinions. In particular, we observe (1) states in which the mean node and mean group opinions are different and (2) excitable and oscillatory opinion dynamics. The excitable and oscillator dynamics (see Sec. V) arise only when the dyadic degree and triadic degree are not fully correlated (i.e., when  $r < 1$ ).

#### IV. GROUP–NODE DISCORDANCE

An important feature of our opinion model is that it admits solutions in which the mean opinion of the nodes differs significantly from the mean opinion of the groups. We refer to these solutions as *group–node discordance states*. These states can model situations in which a social organization (or other social group) has a different official stance than the individuals who comprise that organization. In our model, we measure the discordance of a solution by calculating

$$D(V^*, Y^*) = |V^* - Y^*|, \quad (27)$$

and we say that a group–node discordance state occurs when  $D(V^*, Y^*) > 0$ . In particular, when  $D(V^*, Y^*) = 1$ , the system has the maximum possible discordance; when  $D(V^*, Y^*) = 0$ , there is no discordance.

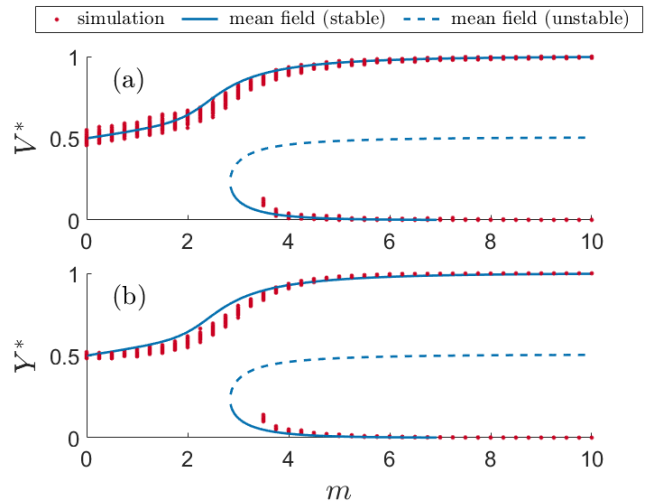


FIG. 2: An example of a bifurcation of the fixed points for completely correlated dyadic and triadic degrees (i.e.,  $r = 1$ ) in simulations of our stochastic opinion model (1) and (2) and solutions of our reduced mean-field equations (23) for the parameter values  $a = b = c = d = \mu = 0.5$  and  $\gamma = 4$ . We show the values of (a)  $V^*$  and (b)  $Y^*$  that we obtain from the mean-field equations (solid and dashed curves) and from means of 100 simulations of our stochastic opinion model (dots) with initial conditions  $\{(i/9, j/9) | i \in \{0, 1, \dots, 9\}, j \in \{0, 1, \dots, 9\}\}$ .

To explore how group–node discordance states can occur due to how group opinions are influenced (i.e., for different values of  $c$  and  $d$ ), we plot  $D(V^*, Y^*)$  versus the node–opinion influence parameter  $a$  (with  $a = b$ ) for the mean of  $V^*$  and  $Y^*$  from 16 independent simulations of the stochastic opinion model (1)–(2) and a numerical solution of the fixed-point equations (24)–(25) for the mean-field approximation (23). In our comparison, we use a single realization of a configuration-model hypergraph with  $N = 2000$  nodes,  $\langle k \rangle = \langle q \rangle = 20$ , and  $\gamma = 4$  for both  $m = 4$  and  $\mu = 0.5$  [see Fig. 3(a)] and  $\mu = 0.25$  [see Fig. 3(b)]. The initial conditions  $(u_1, u_2)$  in the 16 independent simulations are evenly spaced in the unit square (i.e.,  $\{(i/3, j/3) | i \in \{0, 1, 2, 3\}, j \in \{0, 1, 2, 3\}\}$ ). For  $\mu = 0.5$ , we obtain more group–node discordance [i.e., larger values of  $D(V^*, Y^*)$ ] when the node parameters  $a$  and  $b$  are very different from the hyperedge parameters  $c$  and  $d$ . We see this in Fig. 3(a) for  $c = d = 0.1$  (red solid curve and open circles) and  $c = d = 0.9$  (orange solid curve and open squares). In both Fig. 3(a) and Fig. 3(b), the maximum discordance occurs when  $a + b$  is on the opposite side of  $\mu$  as  $c + d$ , indicating that the node and hyperedge opinions experience opposite biases. When  $c = 0.1$  and  $d = 0.9$ , we observe a more uniform discordance in the system, with a small decrease near  $a = b = 0.5$ . When  $\mu = 0.25$  [see Fig. 3(b)] for  $c = d = 0.1$  and  $c = d = 0.9$ , we obtain the same general trend. The group–node discordance states arise most



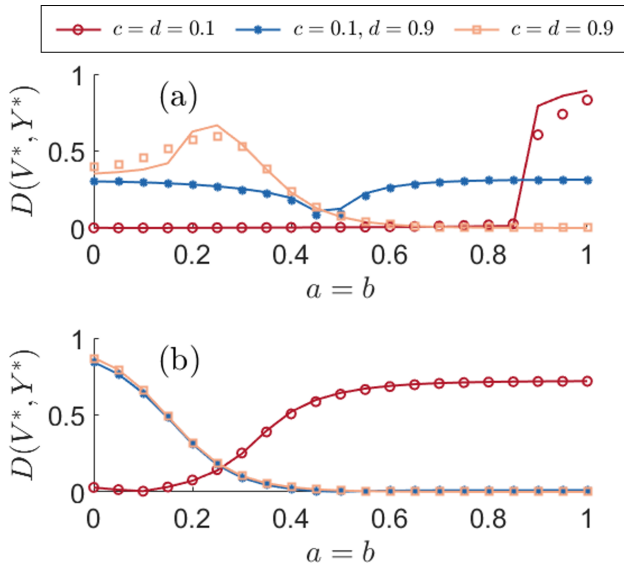


FIG. 3: We plot  $D(V^*, Y^*)$  versus the node-opinion influence parameter  $a$ , with  $a = b$ , for a single numerical solution  $(V^*, Y^*) = (F(V^*), G(V^*))$  of Eqs. (26) (solid curves) and the mean of 16 independent simulations of the stochastic opinion model (1)–(2) for a single configuration-model hypergraph with  $N = 2000$  nodes, mean degrees  $\langle k \rangle = \langle q \rangle = 20$ ,  $m = 4$ ,  $\gamma = 4$ , and several values of  $c$  and  $d$ . We consider (a)  $\mu = 0.5$  and (b)  $\mu = 0.25$ . The initial conditions in the 16 independent simulations are  $\{(i/3, j/3) \mid i \in \{0, 1, 2, 3\}, j \in \{0, 1, 2, 3\}\}$ .

prominently when  $c + d < \mu < a + b$  or  $a + b < \mu < c + d$ . For  $\mu = 0.5$  [see Fig. 3(a)], the transition to a group-node discordance state for  $c = d = 0.1$  appears to be discontinuous; for  $\mu = 0.25$  [see Fig. 3(b)], the transition to such a state is continuous.

We also explore how the width (which is proportional to  $1/m$ ) of the sigmoid transition region can affect the onset of group-node discordance states. To do this, we plot  $D(V^*, Y^*)$  versus  $m$  for several values of  $a$ ,  $b$ ,  $c$ , and  $d$ . We compute  $D(V^*, Y^*)$  using the mean of  $V^*$  and  $Y^*$  from 16 independent simulations of the stochastic opinion model (1)–(2) and a numerical solution of the fixed-point equations (24)–(25) of the reduced mean-field approximation (23). In our comparison, we use a single realization of a configuration-model hypergraph with  $N = 2000$  nodes,  $\langle k \rangle = \langle q \rangle = 20$ , and  $\gamma = 4$ . For each simulation of the stochastic opinion model [see Eqs. (1)–(2)], the initial conditions  $(u_1, u_2)$  in the 16 independent simulations are evenly spaced in the unit square (i.e.,  $\{(i/3, j/3) \mid i \in \{0, 1, 2, 3\}, j \in \{0, 1, 2, 3\}\}$ ). We consider both  $\mu = 0.5$  [see Fig. 4(a)] and  $\mu = 0.25$  [see Fig. 4(b)]. In this example, we explore the effect of varying the width parameter  $m$  for different values of the node parameters ( $a$  and  $b$ ) and the hyperedge parameters ( $c$  and  $d$ ). When  $a = b = c = d = 0.5$  (closed blue circles), the parameter  $m$  has a minimal effect and  $D(V^*, Y^*)$  remains close

to 0, indicating very little group-node discordance. For both  $a = b = 0.2$ ,  $c = d = 0.8$  (open red circles) and  $a = b = 0.8$ ,  $c = d = 0.2$  (open orange squares), the group-node discordance has a maximum at an intermediate value of  $m$ . Lastly, there is an interesting difference between the cases  $\mu = 0.5$  [see Fig. 4(a)] and  $\mu = 0.25$  [see Fig. 4(b)]. When  $a = b = 0.8$  and  $c = d = 0.2$ , there is a seemingly discontinuous transition from discordance to non-discordance for  $\mu = 0.5$ ; however, the transition is continuous for  $\mu = 0.25$ .

As one can see in Figs. 3 and 4, the dependence of group-node discordance on the model parameters is very rich, including discontinuous transitions and nonmonotonic dependence. We leave further analysis of this dependence for future work.

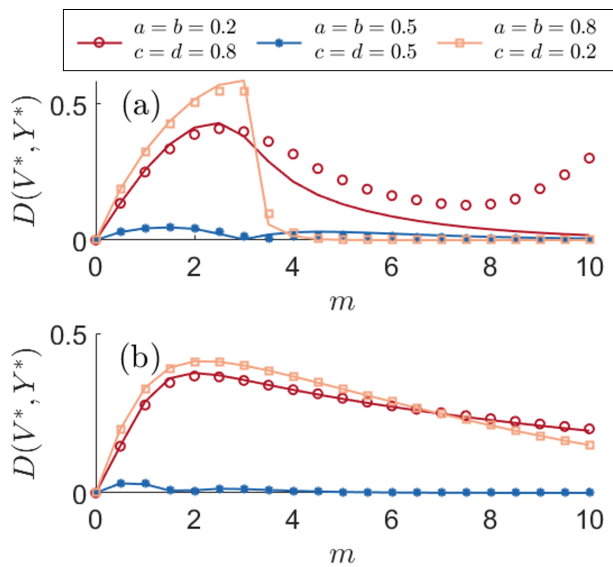


FIG. 4: We plot  $D(V^*, Y^*)$  versus the sigmoid width parameter  $m$  for a single numerical solution  $(V^*, Y^*) = (F(V^*), G(V^*))$  of Eqs. (26) (solid curves) and the mean of 16 independent simulations of the stochastic opinion model (1)–(2) for a single realization of a configuration-model hypergraph with  $N = 2000$  nodes, mean degree  $\langle k \rangle = \langle q \rangle = 20$ ,  $\gamma = 4$ , and several values of  $a$ ,  $b$ ,  $c$ , and  $d$ . We consider (a)  $\mu = 0.5$  and (b)  $\mu = 0.25$ . The initial conditions in the 16 independent simulations are  $\{(i/3, j/3) \mid i \in \{0, 1, 2, 3\}, j \in \{0, 1, 2, 3\}\}$ .

## V. EXCITABLE AND OSCILLATORY DYNAMICS

Our opinion model also has excitable and oscillatory opinion dynamics. To illustrate these dynamics, we simulate both the stochastic opinion model (1)–(2) and the mean-field approximation (22) with the parameters  $(a, b, c, d) = (1, -0.5, 0.25, 0.25)$  and  $(m, \mu) = (8, 0.25)$ . In this regime, the nodes are influenced considerably by

the opinions of their neighboring nodes ( $a = 1$ ), nodes reject the opinions of their groups ( $b = -0.5$ ), groups are influenced equally by their constituent nodes and their own opinions ( $c = d = 0.25$ ), and both nodes and groups have a small sigmoidal-function inflection point ( $\mu = 0.25$ ).

We first suppose that the dyadic and triadic degrees are completely correlated (i.e.,  $r = 1$ ). This situation yields excitable dynamics, in which a dynamical system is initially at a locally stable equilibrium, but — for a sufficiently large perturbation (which is often called a “stimulus”) — experiences a large excursion through phase space before returning to the equilibrium [32, 33]. Excitable dynamics are common in neuronal and cardiac systems, and they are often associated with a system being near to a bifurcation from a resting state to a sustained spiking or oscillatory behavior [32, 33, 75]. In Fig. 5, we show the expected node fraction  $V^t$  (red) and the expected triangle fraction  $Y^t$  (blue) from numerical simulations of Eqs. (1)–(2) for the aforementioned parameter values and a configuration-model hypergraph with  $N = 1000$  nodes and an approximate power-law hyperdegree distribution with  $\gamma = 4$ . The dashed curves show the fixed-point solution that we obtain by solving Eqs. (24)–(25). One can see that the expected node fraction  $V^t$  remains close to the fixed-point solution for a short time before it increases sharply and then subsequently decreases and returns approximately to the fixed-point solution. The expected triangle fraction  $Y^t$  has the same behavior; its dynamics follow  $V^t$  with a short delay. We use the term *opinion pulses* for these spikes in  $V^t$  and  $Y^t$ .

In Fig. 6, we show  $V^t$  as a function of time in simulations of Eqs. (1)–(2) (top) and the mean-field equations (22) (bottom). For the mean-field equations, we introduce a stimulus at time  $t = 200$  by increasing both  $U^t$  and  $V^t$  by 0.2 (vertical arrow). Following the stimulation, the mean-field equations successfully yield a single opinion pulse, which resembles the ones that we observe in our simulations of our stochastic opinion model (1)–(2), in which finite-size fluctuations seemingly provide a stimulus.

As we decrease the correlation  $r$  between the dyadic and triadic degrees, the opinion pulses become more frequent until they eventually become self-sustained oscillations. We show an example of such oscillations in Fig. 7, in which we plot  $V^t$  (blue) and  $Y^t$  (red) as a function of time from a single simulation of our stochastic opinion model (1)–(2) (see the top panel) and the mean-field equations (22) (see the bottom panel) for  $r = 0.15$ . The mean-field equations again successfully reproduce the qualitative behavior of our stochastic opinion model.

One can use the mean-field equations (22) to understand the transition from excitable to oscillatory dynamics as the correlation  $r$  decreases. When  $r = 1$ , the mean-field map (22) has three fixed points [see Fig. 8(a)]. We obtain these fixed points using root-finding methods and assess their stability by examining the eigenvalues of the

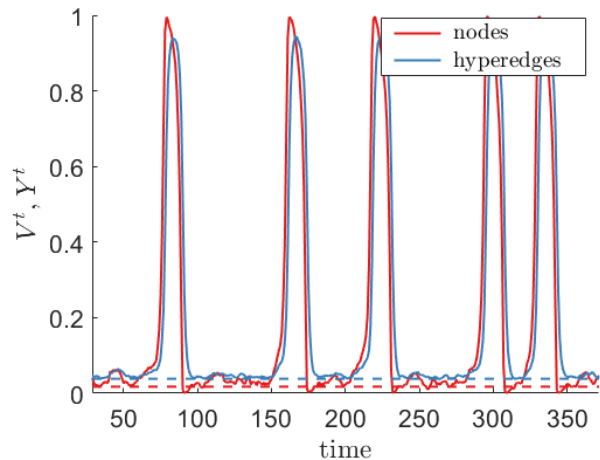


FIG. 5: An example of short-term opinion pulses in a single simulation of our stochastic opinion model (1)–(2) with parameter values  $a = 1$ ,  $b = -0.5$ ,  $c = d = 0.25$ ,  $\mu = 0.25$ , and  $m = 8$  for a configuration-model hypergraph with completely correlated dyadic and triadic degrees (i.e.,  $r = 1$ ) that we draw from an approximate power-law distribution with exponent  $\gamma = 4$ . The dashed lines show the fixed points that we obtain by solving Eqs. (24)–(25).

Jacobian matrix of the mean-field map (22). We compute the Jacobian matrix numerically using the “Adaptive Robust Numerical Differentiation” package for MATLAB [76]. One of the fixed points [the blue disk in Fig. 8(a,b)] is linearly stable. A nearby fixed point [the open green circle in Fig. 8(a)–(c)] is a saddle, and the third fixed point [the red star in Fig. 8(a)–(c)] is an unstable spiral. When the state of the mean-field system (22) is close to the stable fixed point and is perturbed so that it crosses the stable manifold of the saddle, it makes an excursion through phase space. It gets close to the unstable spiral and then returns to the stable fixed point, completing an opinion pulse. In Fig. 8(a), we show an example of such a trajectory in phase space. As we decrease  $r$ , the stable and saddle fixed points approach each other [see Fig. 8(b)], allowing one to create an opinion pulse with a smaller stimulus. Eventually, these two fixed points collide in a saddle–node bifurcation, resulting in oscillatory behavior [see Fig. 8(c)].

The mean-field equations (22) are an approximation of our stochastic opinion model (1)–(2), so we expect a similar bifurcation to exist in the stochastic opinion model. Therefore, we believe that the occurrence of a saddle–node bifurcation and the existence of a locally unstable spiral near the point where the stable node and saddle merge provides a good explanation of the formation of the excitable and oscillatory dynamics in both the mean-field approximation (22) and the stochastic opinion model (1)–(2).

We have seen that decreasing the correlation between

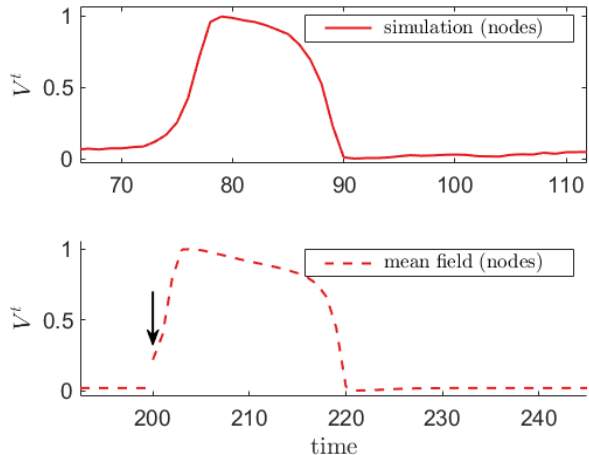


FIG. 6: We compare a single pulse of  $V^t$  for (top) a single simulation of our stochastic opinion model (1)–(2) and (bottom) the mean-field equations (23) for the parameter values  $a = 1$ ,  $b = -0.5$ ,  $c = d = 0.25$ ,  $\mu = 0.25$ , and  $m = 8$  for a hypergraph with completely correlated dyadic and triadic degrees that we draw from an approximate power-law distribution with exponent  $\gamma = 4$ . We apply a stimulus (which is indicated by the black arrow) of  $(\delta V, \delta U, \delta Y) = (0.2, 0.2, 0)$  to the mean-field equations to induce an excitation at time  $t = 200$ .

dyadic and triadic degrees can result in transitions from excitable dynamics to oscillatory dynamics. To explore the effect of hypergraph structure on opinion dynamics more systematically, we consider different values of both the correlation coefficient  $r$  and the exponent  $\gamma$  of the approximate power-law degree distribution. We compute the difference

$$\mathcal{H}(V^t, \mathcal{I}) := \max_{\mathcal{I}}(V^t) - \min_{\mathcal{I}}(V^t), \quad (28)$$

between the maximum and minimum values of  $V^t$  in an interval  $\mathcal{I}$ . A fixed-point solution of Eqs. (22) gives  $\mathcal{H}(V^t, \mathcal{I}) \approx 0$  if we choose an interval  $\mathcal{I}$  after the transient dynamics have dissipated. Oscillations and opinion pulses both yield  $\mathcal{H}(V^t, \mathcal{I}) > 0$ . In principle, one can also distinguish between pulses and oscillations by sliding the interval  $\mathcal{I}$  and/or varying its length, but we have not examined these approaches. In Fig. 9, we plot  $\mathcal{H}(V^t, \mathcal{I})$  versus the power-law exponent  $\gamma$  from Eq. (11) and the correlation coefficient  $r$  for dyadic and triadic degrees in the interval  $\mathcal{I} = [100, 400]$ , which seems to provide adequate time for the transient behavior to disappear. For each pair  $(r, \gamma)$ , we simulate our stochastic opinion model (1)–(2) and the mean-field equations (22) to obtain  $\mathcal{H}$  from Eq. (28). For the stochastic opinion model, we construct  $\mathcal{H}$  by taking a mean of 25 independent simulations for the same hypergraph. The initial conditions  $(u_1, u_2)$  in the 25 independent simulations are evenly spaced in the unit square (i.e.,  $\{(i/4, j/4) \mid i \in \{0, 1, \dots, 4\}, j \in \{0, 1, \dots, 4\}\}$ ). For the mean-field equations (22), we

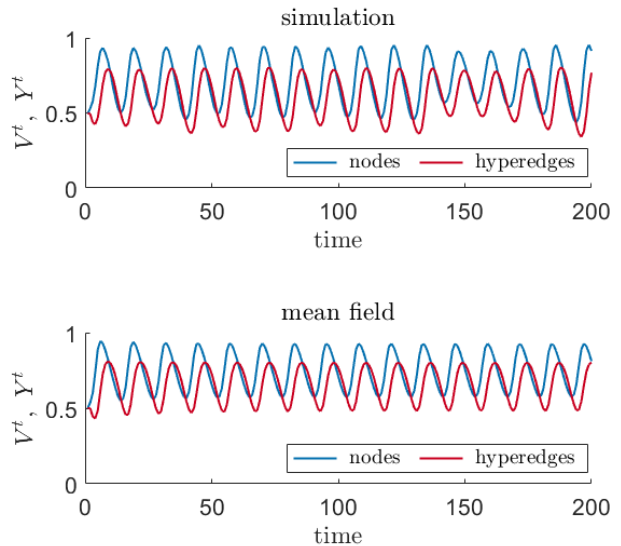


FIG. 7: An example of the oscillatory dynamics in (top) a single simulation of our stochastic opinion model (1)–(2) and (bottom) the mean-field equations (22) for parameter values  $a = 1$ ,  $b = -0.5$ ,  $c = d = 0.25$ ,  $\mu = 0.25$ ,  $m = 8$ ,  $r = 0.15$ , and  $\gamma = 3.8$ . The initial conditions of the stochastic opinion model are  $(u_1, u_2) = (0.5, 0.5)$ , and the initial conditions of the mean-field equations are  $(V^0, U^0, Y^0) = (0.5, 0.5, 0.5)$ .

take a mean of  $\mathcal{H}$  of 25 independent simulations with initial conditions  $(V^0, U^0, Y^0) \in \{(i/4, i/4, j/4) \mid i \in \{0, 1, \dots, 4\}, j \in \{0, 1, \dots, 4\}\}$ . This ensures that  $V^0 = U^0$  (see Sec. III) and hence that the initial conditions of the mean-field equations are as similar as possible to the initial conditions of the stochastic opinion model. In the top panel, we plot  $\mathcal{H}$  from simulations of the stochastic opinion model (1)–(2). In the bottom panel, we plot  $\mathcal{H}$  from the mean-field equations (22). For a given value of the correlation coefficient  $r$ , nonstationary dynamics occur only for a narrow range of power-law exponents, illustrating that oscillatory and excitable dynamics are very sensitive to network structure. A stronger correlation between dyadic and triadic degrees (i.e., a larger  $r$ ) requires a smaller value of  $\gamma$  (i.e., a more heterogeneous network) for nonstationary dynamics to occur. Interestingly, perfectly correlated dyadic and triadic degrees (i.e.,  $r = 1$ ), which reduce the dimensionality of the mean-field equations (22) from 3 to 2, suppress the oscillatory dynamics. Observe that the yellow band [which indicates a large value of  $\mathcal{H}(V^t, \mathcal{I})$ ] in the bottom panel of Fig. 9 does not extend to  $r = 1$ .

Despite their qualitative similarities, the dynamics of the mean-field equations [see the bottom panel of Fig. 9] differs from those of the stochastic opinion model [see the top panel of Fig. 9]. As we discussed above, although the mean-field equations (22) support excitable dynamics, we

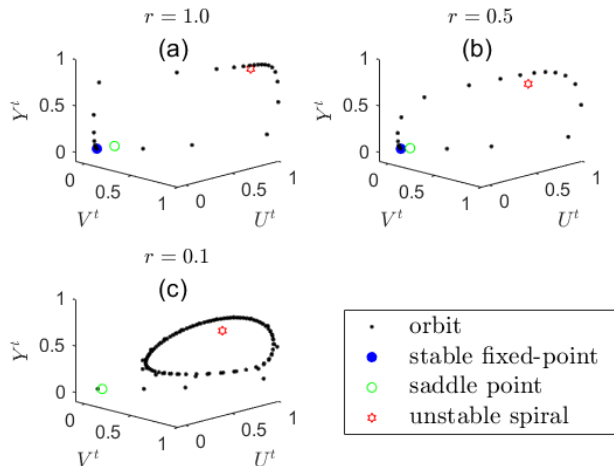


FIG. 8: The phase-space trajectory of a solution of the mean-field equations (22) with a perturbation  $(\delta V, \delta U, \delta Y) = (0.25, 0.25, 0)$  for a hyperdegree distribution with correlations between the dyadic and triadic degrees of (a)  $r = 1$ , (b)  $r = 0.5$ , and (c)  $r = 0.1$ . The merging of stable and unstable fixed points near an unstable spiral leads to the transition from excitable to oscillatory dynamics. The parameter values are  $a = 1$ ,  $b = -0.5$ ,  $c = d = 0.25$ ,  $\mu = 0.25$ ,  $m = 8$ ,  $\gamma = 4$ , and  $\langle k \rangle = \langle q \rangle = 20$  in the mean-field equations (22).

need some type of stimulation to obtain opinion pulses. To mimic the effect of finite-size fluctuations, which are absent in the deterministic mean-field equations (22), we introduce a stochastic term. We consider the equations

$$\begin{aligned}
 V^{t+1} &= \sum_k \sum_q \frac{k\mathcal{P}(k,q)}{\langle k \rangle} f\left(\frac{ak}{\langle k \rangle} V^t + \frac{bq}{\langle q \rangle} Y^t\right) + \sigma_1^t, \\
 U^{t+1} &= \sum_k \sum_q \frac{q\mathcal{P}(k,q)}{\langle q \rangle} f\left(\frac{ak}{\langle k \rangle} V^t + \frac{bq}{\langle q \rangle} Y^t\right) + \sigma_2^t, \\
 Y^{t+1} &= Y^t f(cU^t + d) + (1 - Y^t)f(cU^t).
 \end{aligned}
 \tag{29}$$

In Eq. (29), we draw  $\sigma_1^t$  and  $\sigma_2^t$  uniformly at random from the interval  $[0, M]$  at each time step. These small stochastic perturbations act as a repeated small stimulus to the system. Our decision to not include a random stimulus to  $Y^t$  arises from our observation that the fluctuations in the fraction of hyperedges with opinion 1 is smaller than the fluctuations in the fraction of nodes with opinion 1. This is the case because a hypergraph from the employed random-hypergraph model has many more hyperedges than nodes. Specifically, there are approximately  $N\langle q \rangle/3$  hyperedges in an  $N$ -node hypergraph.

In the middle panel of Fig. 9, we show  $\mathcal{H}$  from the mean-field equations with stochastic fluctuations (29) with an upper bound of  $M = 0.036$  on the stochastic noise. We are not attempting to accurately reproduce the finite-size fluctuations of our stochastic opinion model (1)–(2). Instead, we seek to demonstrate that

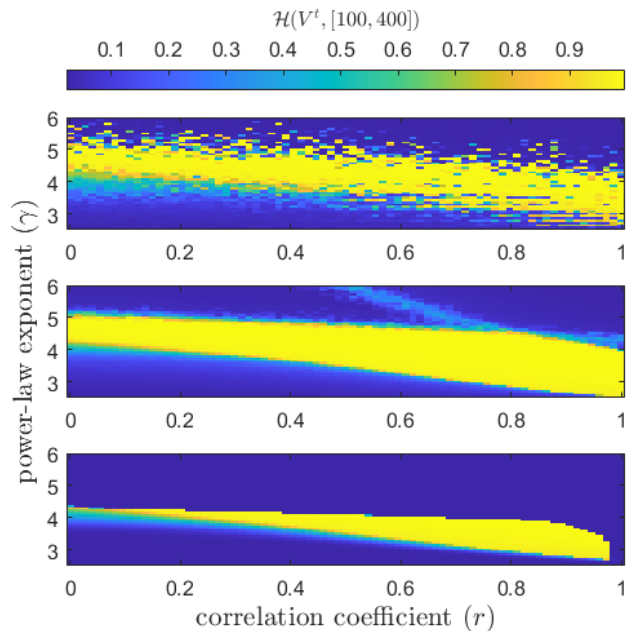


FIG. 9: A heat map of  $\mathcal{H}(V^t, \mathcal{I}) = \max_{\mathcal{I}}(V^t) - \min_{\mathcal{I}}(V^t)$  for (top) a mean of 25 independent simulations of our stochastic opinion model (1)–(2) with initial conditions  $(u_1, u_2) \in \{(i/4, j/4) \mid i \in \{0, 1, \dots, 4\}, j \in \{0, 1, \dots, 4\}\}$ ; (middle) the mean of 25 independent simulations of the mean-field equations with stochastic fluctuations (29) with initial conditions  $(V^0, U^0, Y^0) \in \{(i/4, i/4, j/4) \mid i \in \{0, 1, \dots, 4\}, j \in \{0, 1, \dots, 4\}\}$ ; and (bottom) a mean of 25 independent simulations of the original mean-field equations (22) with initial conditions  $(V^0, U^0, Y^0) \in \{(i/4, i/4, j/4) \mid i \in \{0, 1, \dots, 4\}, j \in \{0, 1, \dots, 4\}\}$ . The horizontal axis is the correlation coefficient  $r$ , and the vertical axis is the power-law exponent  $\gamma$ . In these simulations, we use a single realization of a configuration-model hypergraph and the parameter values  $a = 1$ ,  $b = -0.5$ ,  $c = d = 0.25$ ,  $\mu = 0.25$ , and  $m = 8$ .

the mean-field description (22), when augmented with stochastic fluctuations, can produce excitable and oscillatory dynamics that are qualitatively similar to those that we obtain from simulations of our stochastic opinion model (1)–(2).

## VI. CONCLUSIONS AND DISCUSSION

We introduced and analyzed a stochastic model of opinion dynamics in which both nodes and groups of nodes have a binary opinion. Importantly, this polyadic opinion model includes novel dynamics that result directly from polyadic interactions. We showed that our model supports a richer repertoire of qualitative dynamics than models in which only nodes have opinions. In particular, our opinion model has both excitable dynamics (in which brief but strong opinion swings arise from

perturbations of a fixed point) and oscillatory dynamics (in which the mean opinions of the nodes and hyperedges have self-sustained oscillations). The excitable dynamics of our system share qualitative similarities with the dynamics of social fads [34]. In particular, the behavior appears initially in a small number of individuals (or via external perturbation for our mean-field approximation), experiences a surge that affects the majority of the system, and then quickly dies out. Our opinion model also possesses group–node discordance states, in which nodes and groups have contradictory opinions. Simulations of our stochastic opinion model and the mean-field approximation both reveal that the excitable and oscillatory dynamics depend significantly on network structure (in particular, on dyadic degrees, polyadic degrees, and the correlation between them).

There are many interesting ways to extend our opinion model. As with all models of opinion dynamics, we greatly simplified human dynamics (or the dynamics between other animals) to formulate a mathematically and computationally tractable model that one can study systematically. For example, we assumed that opinions are binary, that interactions occur through a known and time-independent hypergraph, and that the evolution of the opinions obeys precise mathematical rules. It is worth relaxing our various assumptions and exploring the consequences of doing so.

One way to generalize our model is to incorporate various heterogeneities, including in the interaction strengths (e.g., some groups or nodes may be more influential than others) and in the shapes of the sigmoidal functions (e.g., some nodes may be more likely than others to change their opinions). For simplicity, we also limited our study to groups of size 3. As we illustrated in our paper, the

dynamics that result from considering only groups of size 3 is already very rich, but it is reasonable to expect that some phenomena occur only in networks with heterogeneous group sizes. For example, perhaps an opinion can propagate from small groups to large groups (or vice versa). Just as the degree distribution of a graph can significantly influence the qualitative behavior of dynamical processes on it [65, 77], we expect that the hyperedge-size distribution (along with hyperdegree distributions) influences the qualitative behavior of dynamical processes on a hypergraph. In our study, we also neglected interactions between groups, which are likely to introduce additional interesting dynamics. Another potentially interesting extension of our model is the inclusion of node self-influence, as individuals typically have some conviction in their prior beliefs. Additionally, although our mean-field approximation adequately reproduced the observed dynamics and provided some theoretical insights, it is based on the assumption that the hypergraph that describes the groups and the nodes is generated by a configuration model. It is worthwhile to extend our mean-field approximations to stochastic-block-model hypergraphs with assortative mixing (which can encode homophily) [67] and community structure [78–80].

#### ACKNOWLEDGMENTS

JGR acknowledges support from NSF Grant DMS-2205967. MAP was funded in part by the National Science Foundation (grant number 1922952) through their program on Algorithms for Threat Detection. We thank Zachary Kilpatrick, Ekaterina Landgren, Nicholas Landry, James Meiss, and Nancy Rodríguez for helpful comments.

- 
- [1] I. V. Kozitsin, Opinion dynamics of online social network users: a micro-level analysis, *The Journal of Mathematical Sociology* **47**, 1 (2023).
  - [2] Q. Zha, G. Kou, H. Zhang, H. Liang, X. Chen, C.-C. Li, and Y. Dong, Opinion dynamics in finance and business: A literature review and research opportunities, *Financial Innovation* **6**, 44 (2020).
  - [3] J. Fernández-Gracia, K. Suchecki, J. J. Ramasco, M. San Miguel, and V. M. Eguíluz, Is the voter model a model for voters?, *Physical Review Letters* **112**, 158701 (2014).
  - [4] D. A. Siegel, Social networks and collective action, *American Journal of Political Science* **53**, 122 (2009).
  - [5] L. Horstmeyer and C. Kuehn, Adaptive voter model on simplicial complexes, *Physical Review E* **101**, 022305 (2020).
  - [6] G. Deffuant, D. Neau, F. Amblard, and G. Weisbuch, Mixing beliefs among interacting agents, *Advances in Complex Systems* **3**, 87 (2000).
  - [7] L. Neuhäuser, A. Mellor, and R. Lambiotte, Multibody interactions and nonlinear consensus dynamics on networked systems, *Physical Review E* **101**, 032310 (2020).
  - [8] A. Hickok, Y. Kureh, H. Z. Brooks, M. Feng, and M. A. Porter, A bounded-confidence model of opinion dynamics on hypergraphs, *SIAM Journal on Applied Dynamical Systems* **21**, 1 (2022).
  - [9] A. Srivastava, C. Chelmiss, and V. K. Prasanna, Computing competing cascades on signed networks, *Social Network Analysis and Mining* **6**, 82 (2016).
  - [10] C. Toccaceli, L. Milli, and G. Rossetti, Opinion dynamic modeling of fake news perception, in *Complex Networks & Their Applications IX. COMPLEX NETWORKS 2020*, edited by R. M. Benito, C. Cherifi, H. Cherifi, E. Moro, L. Rocha, and M. Sales-Pardo (Springer-Verlag, Heidelberg, Germany, 2020) pp. 370–381.
  - [11] S. Maletić and M. Rajković, Consensus formation on a simplicial complex of opinions, *Physica A: Statistical Mechanics and its Applications* **397**, 111 (2014).
  - [12] R. Sahasrabudde, L. Neuhäuser, and R. Lambiotte, Modelling non-linear consensus dynamics on hypergraphs, *Journal of Physics: Complexity* **2**, 025006 (2021).
  - [13] F. Baumann, P. Lorenz-Spreen, I. M. Sokolov, and M. Starnini, Modeling echo chambers and polarization



- dynamics in social networks, *Physical Review Letters* **124**, 048301 (2020).
- [14] H. Z. Brooks, P. S. Chodrow, and M. A. Porter, Emergence of polarization in a sigmoidal bounded-confidence model of opinion dynamics, *SIAM Journal on Applied Dynamical Systems* **23**, 1442 (2024).
- [15] A. Sîrbu, V. Loreto, V. D. P. Servedio, and F. Tria, Opinion dynamics: Models, extensions and external effects, in *Participatory Sensing, Opinions and Collective Awareness*, edited by V. Loreto, M. Haklay, A. Hotho, V. D. Servedio, G. Stumme, J. Theunis, and F. Tria (Springer International Publishing, Cham, Switzerland, 2017) pp. 363–401.
- [16] H. Noorazar, K. R. Vixie, A. Talebanpour, and Y. Hu, From classical to modern opinion dynamics, *International Journal of Modern Physics C* **31**, 2050101 (2020).
- [17] H. Olsson and M. Galesic, Analogies for modeling belief dynamics, *Trends in Cognitive Sciences* (2024), in press, available at <https://doi.org/10.1016/j.tics.2024.07.001>.
- [18] Z. Xie, X. Song, and Q. Li, A review of opinion dynamics, in *Theory, Methodology, Tools and Applications for Modeling and Simulation of Complex Systems: 16th Asia Simulation Conference and SCS Autumn Simulation Multi-Conference, AsiaSim/SCS AutumnSim 2016, Beijing, China, October 8–11, 2016, Proceedings, Part IV 16* (Springer-Verlag, Heidelberg, Germany, 2016) pp. 349–357.
- [19] M. H. DeGroot, Reaching a consensus, *Journal of the American Statistical Association* **69**, 118 (1974).
- [20] P. Clifford and A. Sudbury, A model for spatial conflict, *Biometrika* **60**, 581 (1973).
- [21] R. A. Holley and T. M. Liggett, Ergodic theorems for weakly interacting infinite systems and the voter model, *The Annals of Probability* **3**, 643 (1975).
- [22] S. Redner, Reality-inspired voter models: A mini-review, *Comptes Rendus Physique* **20**, 275 (2019).
- [23] S. Galam, Minority opinion spreading in random geometry, *The European Physical Journal B* **25**, 403 (2002).
- [24] C. Bernardo, C. Altafini, A. Proskurnikov, and F. Vasca, Bounded confidence opinion dynamics: A survey, *Automatica* **159**, 111302 (2024).
- [25] R. L. Breiger, The duality of persons and groups, *Social forces* **53**, 181 (1974).
- [26] C. Burningham and M. A. West, Individual, climate, and group interaction processes as predictors of work team innovation, *Small Group Research* **26**, 106 (1995).
- [27] G. A. Fine, The hinge: Civil society, group culture, and the interaction order, *Social Psychology Quarterly* **77**, 5 (2014).
- [28] M. Eilert and A. Nappier Cherup, The activist company: Examining a company’s pursuit of societal change through corporate activism using an institutional theoretical lens, *Journal of Public Policy & Marketing* **39**, 461 (2020).
- [29] R. C. Black, R. J. Owens, J. Wedeking, and P. C. Wohlfarth, *US Supreme Court Opinions and Their Audiences* (Cambridge University Press, Cambridge, UK, 2016).
- [30] R. B. Cialdini and N. J. Goldstein, Social influence: Compliance and conformity, *Annual Review of Psychology* **55**, 591 (2004).
- [31] V. Giskevicius, N. J. Goldstein, C. R. Mortensen, R. B. Cialdini, and D. T. Kenrick, Going along versus going alone: When fundamental motives facilitate strategic (non)conformity, *Journal of Personality and Social Psychology* **91**, 281 (2006).
- [32] R. Sepulchre, G. Drion, and A. Franci, *Excitable behaviors* (Springer-Verlag, Heidelberg, Germany, 2018) pp. 269–280.
- [33] E. M. Izhikevich, *Dynamical Systems in Neuroscience* (MIT Press, Cambridge, MA, USA, 2007).
- [34] J. Best, *Flavor of the Month: Why Smart People Fall for Fads* (University of California Press, Oakland, CA, USA, 2006).
- [35] B. E. Aguirre, E. L. Quarantelli, and J. L. Mendoza, The collective behavior of fads: The characteristics, effects, and career of streaking, *American Sociological Review* **53**, 569 (1988).
- [36] F. Battiston, G. Cencetti, I. Iacopini, V. Latora, M. Lucas, A. Patania, J.-G. Young, and G. Petri, Networks beyond pairwise interactions: Structure and dynamics, *Physics Reports* **874**, 1 (2020).
- [37] C. Bick, E. Gross, H. A. Harrington, and M. T. Schaub, What are higher-order networks?, *SIAM Review* **65**, 686 (2023).
- [38] Z. Gao, D. Ghosh, H. A. Harrington, J. G. Restrepo, and D. Taylor, Dynamics on networks with higher-order interactions, *Chaos: An Interdisciplinary Journal of Nonlinear Science* **33**, 040401 (2023).
- [39] R. H. Atkin, *Combinatorial Connectivities in Social Systems: An Application of Simplicial Complex Structures to the Study of Large Organizations* (Springer-Verlag, Heidelberg, Germany, 1977).
- [40] P. A. Abrams, Arguments in favor of higher order interactions, *The American Naturalist* **121**, 887 (1983).
- [41] H. M. Wilbur and J. E. Fauth, Experimental aquatic food webs: Interactions between two predators and two prey, *The American Naturalist* **135**, 176 (1990).
- [42] H. Schaffer and C. Liddell, Adult–child interaction under dyadic and polyadic conditions, *British Journal of Developmental Psychology* **2**, 33 (1984).
- [43] I. Iacopini, G. Petri, A. Barrat, and V. Latora, Simplicial models of social contagion, *Nature Communications* **10**, 2485 (2019).
- [44] N. W. Landry and J. G. Restrepo, The effect of heterogeneity on hypergraph contagion models, *Chaos: An Interdisciplinary Journal of Nonlinear Science* **30**, 103117 (2020).
- [45] L. Neuhäuser, M. T. Schaub, A. Mellor, and R. Lambiotte, Opinion dynamics with multi-body interactions, in *International Conference on Network Games, Control and Optimization. NETGCOOP 2021.*, edited by S. Lasaulce, P. Mertikopoulos, and A. Orda (Springer International Publishing, Cham, Switzerland, 2021) pp. 261–271.
- [46] G. Cencetti, F. Battiston, B. Lepri, and M. Karsai, Temporal properties of higher-order interactions in social networks, *Scientific Reports* **11**, 7028 (2021).
- [47] J. Noonan and R. Lambiotte, Dynamics of majority rule on hypergraphs, *Physical Review E* **104**, 024316 (2021).
- [48] J. Kim, D.-S. Lee, B. Min, M. A. Porter, M. S. Miguel, and K.-I. Goh, Competition between group interactions and nonlinearity in voter dynamics on hypergraphs, arXiv preprint arXiv:2407.11261 (2024).
- [49] L. Hébert-Dufresne, T. M. Waring, G. St-Onge, M. T. Niles, L. Kati Corlew, M. P. Dube, S. J. Miller, N. J. Gotelli, and B. J. McGill, Source-sink behavioural dynamics limit institutional evolution in a group-structured

- society, *Royal Society Open Science* **9**, 211743 (2022).
- [50] G. St-Onge, L. Hébert-Dufresne, and A. Allard, Nonlinear bias toward complex contagion in uncertain transmission settings, *Proceedings of the National Academy of Sciences of the United States of America* **121**, e2312202121 (2024).
- [51] J. St-Onge, G. Burgio, S. F. Rosenblatt, T. M. Waring, and L. Hébert-Dufresne, Paradoxes in the coevolution of contagions and institutions, *Proceedings of the Royal Society B* **291**, 20241117 (2024).
- [52] A. P. Millán, J. J. Torres, and G. Bianconi, Explosive higher-order Kuramoto dynamics on simplicial complexes, *Physical Review Letters* **124**, 218301 (2020).
- [53] R. Ghorbanchian, J. G. Restrepo, J. J. Torres, and G. Bianconi, Higher-order simplicial synchronization of coupled topological signals, *Communications Physics* **4**, 120 (2021).
- [54] T. Carletti, L. Giambagli, and G. Bianconi, Global topological synchronization on simplicial and cell complexes, *Physical Review Letters* **130**, 187401 (2023).
- [55] P. Cisneros-Velarde and F. Bullo, Multi-group SIS epidemics with simplicial and higher-order interactions, *IEEE Transactions on Control of Network Systems* **9**, 695 (2022).
- [56] P. S. Skardal and A. Arenas, Higher order interactions in complex networks of phase oscillators promote abrupt synchronization switching, *Communications Physics* **3**, 218 (2020).
- [57] S. Adhikari, J. G. Restrepo, and P. S. Skardal, Synchronization of phase oscillators on complex hypergraphs, *Chaos: An Interdisciplinary Journal of Nonlinear Science* **33**, 033116 (2023).
- [58] K. Nikolay and M. Svetoslav, *Sigmoid Functions: Some Approximation and Modelling Aspects* (Lambert Academic Publishing, London, UK, 2015).
- [59] A. Bizyaeva, A. Franci, and N. E. Leonard, Nonlinear opinion dynamics with tunable sensitivity, *IEEE Transactions on Automatic Control* **68**, 1415 (2023).
- [60] D. A. Prentice and D. T. Miller, Pluralistic ignorance and the perpetuation of social norms by unwitting actors, *Advances in Experimental Social Psychology* **28**, 161 (1996).
- [61] D. T. Miller and C. McFarland, Pluralistic ignorance: When similarity is interpreted as dissimilarity, *Journal of Personality and Social Psychology* **53**, 298 (1987).
- [62] I. L. Janis, Groupthink, *Psychology Today* **5**, 43 (1971).
- [63] Y. H. Kureh and M. A. Porter, Fitting in and breaking up: A nonlinear version of coevolving voter models, *Physical Review E* **101**, 062303 (2020).
- [64] C. Bicchieri and H. Mercier, Norms and beliefs: How change occurs, in *The Complexity of Social Norms* (Springer-Verlag, Heidelberg, Germany, 2014) pp. 37–54.
- [65] M. E. J. Newman, *Networks*, 2nd ed. (Oxford University Press, Oxford, UK, 2018).
- [66] L. Torres, A. S. Blevins, D. Bassett, and T. Eliassi-Rad, The why, how, and when of representations for complex systems, *SIAM Review* **63**, 435 (2021).
- [67] N. W. Landry and J. G. Restrepo, Hypergraph assortativity: A dynamical systems perspective, *Chaos: An Interdisciplinary Journal of Nonlinear Science* **32** (2022).
- [68] P. S. Chodrow, Configuration models of random hypergraphs, *Journal of Complex Networks* **8**, cnaa018 (2020).
- [69] B. K. Fosdick, D. B. Larremore, J. Nishimura, and J. Ugander, Configuring random graph models with fixed degree sequences, *Siam Review* **60**, 315 (2018).
- [70] M. E. J. Newman, Random graphs with clustering, *Physical Review Letters* **103**, 058701 (2009).
- [71] J. C. Miller, Percolation and epidemics in random clustered networks, *Physical Review E* **80**, 020901 (2009).
- [72] I. Z. Kiss, J. C. Miller, and P. L. Simon, *Mathematics of Epidemics on Networks: From Exact to Approximate Models* (Springer International Publishing, Cham, Switzerland, 2017).
- [73] G. F. de Arruda, A. Aleta, and Y. Moreno, Contagion dynamics on higher-order networks, *Nature Reviews Physics* (2024), available at <https://doi.org/10.1038/s42254-024-00733-0>.
- [74] S. Melnik, M. A. Porter, P. J. Mucha, and J. P. Gleeson, Dynamics on modular networks with heterogeneous correlations, *Chaos: An Interdisciplinary Journal of Nonlinear Science* **24**, 023106 (2014).
- [75] R. Barrio, S. Coombes, M. Desroches, F. Fenton, S. Luther, and E. Pueyo, Excitable dynamics in neural and cardiac systems, *Communications in Nonlinear Science and Numerical Simulation* **86**, 105275 (2020).
- [76] J. D'Errico, Adaptive robust numerical differentiation, available at <https://www.mathworks.com/matlabcentral/fileexchange/13490-adaptive-robust-numerical-differentiation>.
- [77] M. A. Porter and J. P. Gleeson, *Dynamical Systems on Networks: A Tutorial*, Vol. 4 (Springer International Publishing, Cham, Switzerland, 2016) *Frontiers in Applied Dynamical Systems: Reviews and Tutorials*.
- [78] N. W. Landry and J. G. Restrepo, Opinion disparity in hypergraphs with community structure, *Physical Review E* **108**, 034311 (2023).
- [79] C. Kim, A. S. Bandeira, and M. X. Goemans, Stochastic block model for hypergraphs: Statistical limits and a semidefinite programming approach, *arXiv preprint arXiv:1807.02884* (2018).
- [80] S. Cole and Y. Zhu, Exact recovery in the hypergraph stochastic block model: A spectral algorithm, *Linear Algebra and its Applications* **593**, 45 (2020).